Thirsty for a Noninvasive Wearable to Detect Dehydration: A Review

J.-C. Chiao[®], Sen Bing[®], Khengdauliu Chawang[®], and Brian Crowe

n this article, significant clinical needs, methods, and principles for continuous human body hydration-level monitoring are reviewed. Maintaining hydration is critical for physical and mental health. A long-term, continuous, convenient, and accurate wearable device that can monitor whole-body water content to provide real-time feedback is needed, especially for infants, the elderly, and people who have special needs in their tasks and occupations. Noninvasive bioimpedance measurements and microwave sensing techniques suitable for conformable wearables are summarized. Microwave probing with deeper field penetrations into the dermis layer of the skin can provide a better assessment of whole-body water content. Frequency choices for the probing signals, the need for realistic phantoms, and evaluation standards suitable for clinical uses are discussed.

CLINICAL SIGNIFICANCE

Hydration is fundamentally important for our health and well-being. Water is essential for many biological processes, including regulating body temperature, transporting nutrients to cells, and removing waste from the body. Insufficient hydration initially produces mild symptoms that include dry skin and headaches. When lack of hydration becomes acute or continuous in the long term, and significant net water loss is

Digital Object Identifier 10.1109/MAP.2024.3442823 Date of current version: 9 October 2024

EDITOR'S NOTE

This article for the "Bioelectromagnetics" column reviews wearable sensing technologies for monitoring hydration levels. Although natural feedback mechanisms of the body are meant to regulate fluid intake, dehydration is still prevalent, particularly in sensitive populations. With a focus on bioimpedance techniques and microwave measurements through the skin, this article aims to raise awareness in the field and motivate future research.



This column welcomes articles on biomedical applications of Asimina Kiourti electromagnetics, antennas, and propagation in terms of research, education, outreach, and more. If you are interested in contributing, please e-mail me at kiourti.1@osu.edu.

experienced in the body, these essential functions are not performed effectively and can have serious repercussions for

many systems in the body.

Dehydration reduces blood circulation and increases the burden on the heart [1], [2]. In terms of anaerobic capacity [3], dehydration reduces the body's ability to generate force and increases the risk of musculoskeletal damage [4]. Additionally, dehydration can promote muscle cramps and spasms, which can further increase the risk of injury, especially for athletes [5].

Dehydration also affects neurological functions that can compound the impact on motor functions. When the body loses water, the imbalance of electrolytes across neuron membranes for elements such as sodium and potassium can disturb neural pathways and may trigger seizures [6], [7]. Reduction of blood flow due to dehydration also reduces the flow of nutrients and

oxygen to the brain, which impairs cognitive functions and causes mood changes, fatigue, irritability, and confusion [8], [9]. Long-term effects can impact memory and attention as well as the development of certain neurodegenerative diseases, including dementia [10], [11].

When the body is dehydrated, blood flow to the kidneys declines and it adversely impacts the kidneys' ability to filter waste and maintain electrolyte balance, which leads to the accumulation of toxins. Sudden dehydration due to heatstroke and diarrhea/vomiting can lead to acute kidney injury [12]. Longterm dehydration increases circulatory workload, which can lead to small blood vessel damage in the kidneys and cause chronic kidney disease [13], [14]. When the body is dehydrated, there is less fluid to flush out bacteria from the urinary tract, and that increases the risk of urinary tract infection [15], [16].

Early detection of dehydration can help prevent these severe or long-lasting consequences. The urinary system and the sensation of thirst provide feedback mechanisms for regulating hydration in healthy individuals to maintain a balance of fluids in the body. However, for people with diminished feedback mechanisms, such as infants, elderly people, and certain medical patients [17], [18]; people who have to focus steadily on their jobs, such as police, soldiers, and athletes [19]; and outdoor workers who sweat excessively and cannot drink water frequently, such as farmers and construction workers [20], [21], consciously self-monitoring hydration levels can be challenging. Monitoring hydration levels to detect dehydration early on is particularly important for those at a higher risk as mild dehydration can be easily treated simply by increasing fluid intake.

CURRENT STATUS OF HYDRATION MONITORING

Measuring human hydration is difficult. Indirect tracking, nonphysiological methods, and clinical assessments, including qualitative and quantitative means, were summarized in [22]. Currently, various indicators, including urine color, body weight changes, urine-specific gravity, and blood tests [23], [24], [25], [26], are used in clinical settings to monitor hydration levels. A urine color check is not specific, and often patients do not produce sufficient urine. Other methods that can help detect dehydration, however, are not convenient or comfortable and cannot provide timely warning for complication prevention. Particularly, most of the quantitative measurement approaches, although sophisticated, need to be used by skilled workers and under controlled conditions that cannot be preserved in daily uses [22]. This calls for wearable devices that can conveniently and continuously monitor body hydration levels in real time. It would be a valuable tool for many people and help to improve their overall health and well-being.

Electrochemical sensors that detect chemical markers on the skin, and probes that measure dielectric properties by electrical or electromagnetic signals are two attractive options for wearables. Ion-selective electrodes on wearables or textiles were developed to monitor sodium or chlorine in sweat for hydration monitoring, especially during exercise [27], [28], [29]. The sensing mechanisms feature specificity for biomarkers but depend on sweat secretion, so the wearable placement locations on the skin are limited and inconvenient or uncomfortable for wearers. The amount of sweat also influences their accuracy. The sensors may also require consumables, such as enzymes, making them cost more. This article focuses only on electrical and electromagnetic measurements that do not require consumables on sensing electrodes.

Sensing with electrical currents or electromagnetic fields relies on the dielectric properties of the tissues, such as permittivities. To avoid confusion, the term *dielectric constant* refers to the real part of the relative complex permittivity, which is frequency and material dependent. The imaginary part of the relative complex permittivity is related to the electric conductivity or loss tangent of the material, which is also frequency dependent.

BIOIMPEDANCE MEASUREMENTS

Measuring skin impedances with two rigid conductive electrodes in firm contact with the skin has been previously considered to evaluate tissue moisture levels. Tissues can be modeled as equivalent circuits consisting of capacitors and resistors [30]. Water plays an important role as its permittivity is much higher than other materials and it increases electric conductivity by carrying ionic elements, such as electrolytes, crossing cell membranes, between cells, and in blood vessels. Bioimpedances have been used for body composition evaluation, such as fat-free mass and fat mass prediction, along with total body water at 5 kHz [31], 50 kHz [30], [32], and multiple frequencies up to 100 kHz [33]. The prediction equations are based on empirical data from specific populations. These studies conclude that the reactances, which are contributed by capacitances, appear to be essential in the single prediction equations of bioimpedances. The studies also indicate that the choices of frequency and electrodes in impedance measurements reveal different dependencies of considered factors. Dielectric dynamics depend on frequency, so bioimpedance spectroscopy (BIS) can be used to characterize impedance responses under different physiological conditions. It was concluded that extracellular water resistance should be measured at a low frequency, below 1 kHz, due to cell membrane capacitances. However, because signals at 50 kHz and below penetrate only a fraction into intracellular water, the combined effect from extracellular and intracellular water, which is the total body water, should be measured at more than 5 MHz [30].

According to the dielectric properties of the biological cells in [34], [35], [36], and [37], as shown in Figure 1, the alpha dispersion at low frequencies presents very high permittivities to the currents, limiting penetration into the cells, except those through ion channels on the membranes. Thus, the impedance response is mostly from the extracellular water and mainly resistive. For the beta dispersion in the frequency range of 10 kHz-10 MHz, the cellular membranes become charged like capacitors and seem to be electrically shorted as the frequency increases to allow currents to penetrate through the cytoplasm, where the intracellular water is held. Thus, the impedance includes effects from both intra- and extracellular water. Measuring impedances across multiple frequencies by BIS below 100 MHz is useful to reveal more information about the skin as both the permittivity and electric conductivity vary in the frequency band.

CONFORMABLE WEARABLES FOR BIOIMPEDANCE MEASUREMENTS

Using two conductive or gel-based surface electrodes to measure skin impedances has several shortcomings. The contact pressure of rigid or surface electrodes on the elastic skin affects electrical current flows. The repeatability of measurements becomes an issue because of inconsistent contact. Stretching and compression of skin and muscles as well as sweat on the skin's surface at the measurement location also affect electrical

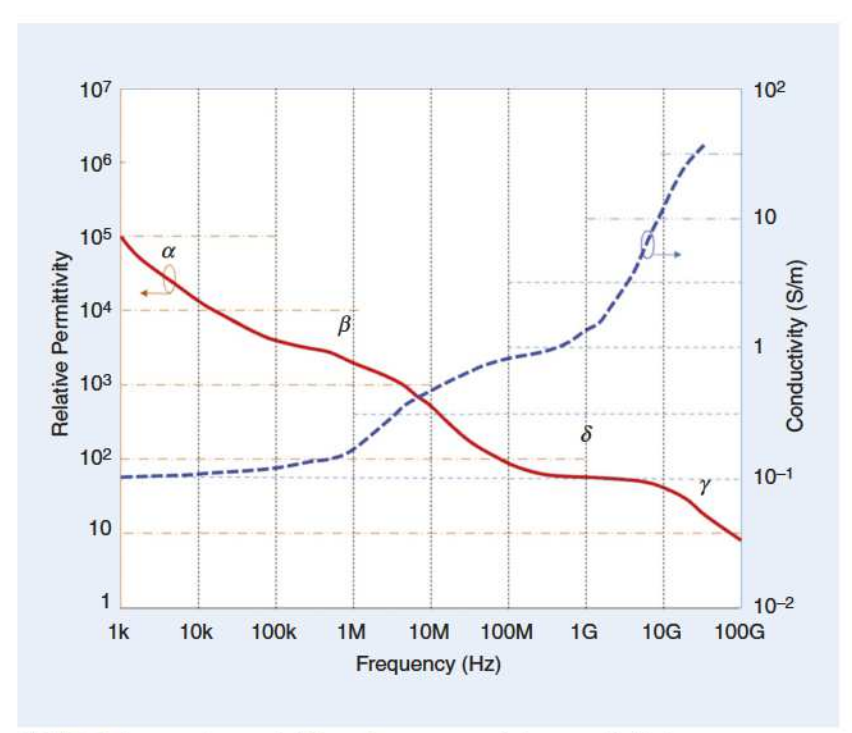


FIGURE 1. An experimental dielectric spectrum of tissues with high water content at 37 °C. The figure is redrawn according to the plots in [34] and [37].

current paths, creating motion artifacts and noises in measurements. For long-term or continuous monitoring, the rigid/surface electrodes can cause irritation or damage to the skin. Thus, planar electrodes on a conformable substrate that can be attached to a small area on the skin become an attractive solution. Planar capacitance sensors commonly include ring and interdigitated types, as shown in Figure 2.

Stretchable skin-like substrates that are integrated with metal patterns of LC resonators have been developed [38]. One wireless epidermal device had dimensions of 11.4 mm \times 24.2 mm. A capacitive sensor with an inner disk of 1 mm in diameter, an outer circular ring

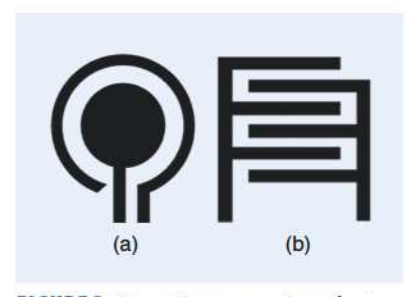


FIGURE 2. Capacitance sensing electrode configurations. (a) A concentric ring/disk and (b) interdigitated fingers.

of 2 mm in diameter, and a 400-µm ring width respond to dielectric constant changes on the skin. The sensor was connected to 4 turns of serpentine-shaped coils acting as an inductor to form a resonator. The resonant frequency shifted from 163 to 176 MHz when the hydration level decreased from 103 to 31, which was defined as an arbitrary unit by a commercial moisture meter (Delfin Moisture Meter SC) as the skin capacitance decreased. The moisture meter was based on a pair of rigid, circular electrodes to measure impedances. The skin hydration levels were varied by applying moisturizing lotions on the skin to prevent transdermal water evaporation.

Another stretchable device implemented three impedance-sensing designs to measure skin impedances [39]. One had a concentric electrode that had an inner disk radius of 150/125 μ m, surrounded by an open-end ring with a radius of 250 μ m and a width of 100 μ m. The second one had 15 metal interdigitated fingers with 20 × 50- μ m² surfaces and a spacing of 20 μ m. Besides these two capacitance sensors, the third design had meander electrodes with two sets of four semicircles, and two arc lines interconnected into a spiral shape to

measure pure resistance changes. All three were integrated into the same substrate with their reference counterparts that had floating ground, so the capacitances were not affected by the skin but responded to other mechanical variations, such as stretching and environmental noises. Experiments were conducted from 15 to 95 kHz by applying moisturizing lotions on the skin against the same commercial moisture sensor mentioned before. As the arbitrary units of the hydration reading increased from 31 to 110, the impedance magnitude decreased by 1.6 $M\Omega$ and the phase changed by 1.18 rad. In the measurement range of frequencies, impedance amplitude and phase changed by 89% and 73%, respectively, at 15 kHz, compared to 34% and 38%, respectively, at 95 kHz. Thus, it was concluded that the increases in skin electric conductivity and permittivity with increasing hydration reduced the overall measured impedances, and skin impedance measurements at lower frequencies provided a higher sensitivity.

As skin impedance measurements conducted by the commercial moisture meter with two electrodes were sensitive to their mechanical pressures on the skin, stretchable and deformable epidermal devices provided clear advantages as they were attached to the skin by van der Waals forces without externally applied forces. A similar sensor was also demonstrated with silver nanowires embedded inside a polydimethylsiloxane matrix as a stretchable wearable [40]. Interdigitated fingers of 20-mm lengths and 2-mm spacings serve as the capacitive sensor that responds to the dielectric constant changes. The frequencies are set in the range of 10-100 kHz to detect the epidermis layer. The equivalent-circuit resistance and capacitance of the epidermis layer at 100 kHz varied in the ranges of $\sim 560-10 \Omega$ and 1-98 nF against the same commercial moisture meter when the readings changed from 15 to 50 and from 42 to 82, respectively, as shown in Figure 2(e) of [40]. In the experiment protocol, skin lotion was applied to the skin for 5 min to achieve a moisturizing effect. Skin resistances and capacitances slowly changed

after applying lotion, and after 20 min they returned to approximately the same impedances as those prior to the lotion application.

THE SKIN

The human skin consists of three basic layers, as shown in Figure 3. The top layer is the epidermis, which acts as a protective barrier to keep pathogens such as bacteria from entering, and resists ultraviolet light from damaging cells. The protective layer also helps regulate temperature and hydration levels. The thickness is roughly 1.5 mm on most parts of the body. Within the epidermis, there are five different layers. The top layer exposed to air is the stratum corneum, which has approximately 20 layers composed of dead cells, called corneocytes, which are closely packed together and surrounded by a matrix of lipids. The thickness and composition of the stratum corneum vary depending on factors such as body part, age, genetics, and environmental exposure. The stratum corneum layer is tough for the purpose of protection. Its thickness significantly affects the sensitivity of a planar capacitive sensor placed on the skin because the other layers that provide permittivity variations due to water content changes are underneath the stratum corneum. A thicker layer reduces the dynamic range of capacitive sensing. Electrical currents from and to the electrodes find the least resistive paths to travel, and they may mostly travel on the top surface of the skin without entering the layers beneath the stratum corneum. The skin's surface conditions in dry or humid environments may produce different results.

The second layer is the dermis, which has a thickness of 1–4 mm, and the bottom layer is the hypodermis, with a wide range of thickness from 1 mm on the eyelids to a few centimeters on the abdomen. The dermis layer contains blood vessels, sweat glands, lymphatic vessels, nerves, and fibroblast cells as connective tissues. The hypodermis layer includes adipose (fatty) tissues, blood vessels, lymphatic vessels, sweat glands, nerves, hair follicles and connective tissues. The cells in these two layers are more sensitive to water con-

tent changes because of the presence of blood and lymphatic vessels and sweat glands. The water content percentages of blood plasma and fat are 91% and 5%-20%, respectively, by weight [41]. At 915 MHz and 2.45 GHz, the dielectric constants at 37 °C are roughly 62 and 60 for blood and 15 and 12 for fat [42]. Their conductivities are 1.41 and 2.04 S/m for blood and 0.35 and 0.82 S/m for fat, respectively. A large contrast in permittivity occurs when water percentage changes. The variation of water percentage in blood has a quicker response to body hydration level, compared to that in cells. Osmosis across cell membranes determines water movement, and water diffusion is slower than blood flow. The higher contrast of the complex permittivity of water in blood/ lymphatic vessels and sweat glands within the dermis and hypodermis layers may provide more sensitive detection of water at the microwave frequency range.

MICROWAVE-BASED HYDRATION SENSING

Microwaves have long been used to detect water content in the atmosphere, soil, and materials due to the rotations and vibrations of water molecules being dipole moments. Remote sensing, particularly by satellites or ground radar,

utilizes L (1-2 GHz), C (4-8 GHz), X (8-2 GHz), and Ku bands (12-18 GHz) for their relatively low atmospheric attenuation and ability to penetrate the soil to interact with water [43]. For example, the European Space Agency's Soil Moisture and Ocean Salinity mission operates at 1.4 GHz [44], [45], while NASA's Soil Moisture Active Passive mission uses dual frequencies at 1.26 and 1.41 GHz [46], [47]. L-band signals are less affected by atmospheric attenuation and surface roughness, while they are sensitive to soil moisture. The C band has been used in the European Earth observation Sentinel-1 satellites for soil moisture at a center frequency of 5.405 GHz [48]. X-band ground and satellite radars are used for high-resolution measurements of precipitation and land imaging [49], [50], [51]. Ku-band scatterometers have been used on the ScatSat-1 satellite for soil moisture measurements [52], [53].

With the analogy of sensing earth soil moisture with microwaves from a satellite, electromagnetic waves can also be implemented to detect water under the skin. The electromagnetic-wave wavelengths in the gigahertz frequency range are on the scale of millimeters, allowing fields to interact within biological cells. A cell contains, on average, 70% water by weight, and water

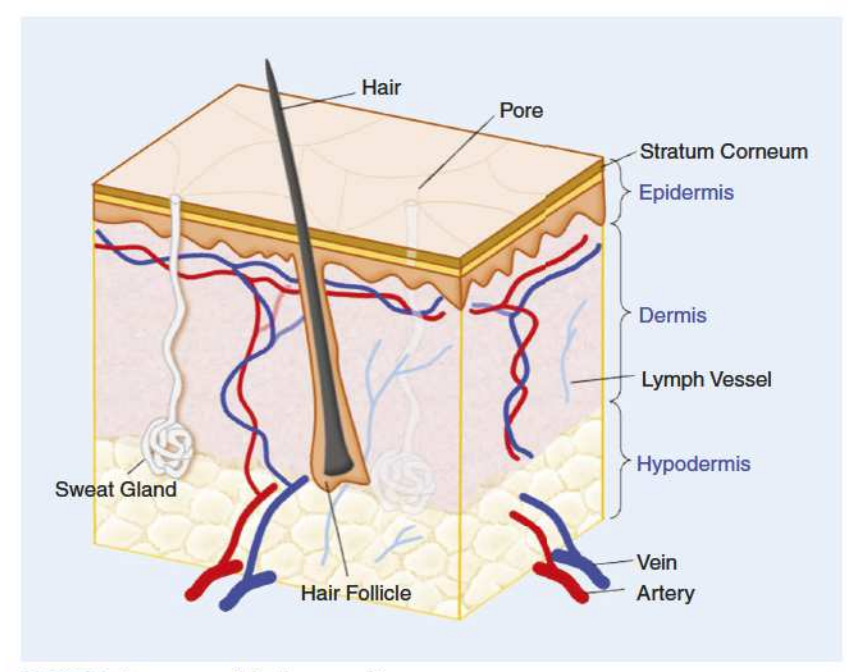


FIGURE 3. Anatomy of the human skin.

is a polar molecule; thus, the complex permittivity in the delta dispersion region at 0.1–5 GHz, shown in Figure 1, is significantly dependent on water content [34], [36]. The interactions between fields and water occur intra- and extracellularly. It should be noted that the fields also interact with charged molecules, such as proteins or enzymes, so the scattered signals may also include such effects. Of course, these biomolecules can also be sensitive to water changes in the cells.

The total body water percentage varies depending on age, body composition, and health. On average, women's body water percentages are in the range of 45%–60%, while men's range is 50%–65%. This means that a person with a weight of 70 kg and a percentage of 60% holds 42 L of total body water [54]. In infants, the range is 75%–78%. Different organs and tissues hold different percentages of water, for example, with total body water of 60%, blood, lungs, heart, and brain have 95%, 83%, 73%, and 73% water, respectively, while bones have 31% [55].

Dielectric dispersion experiments show pure water has a high real-part relative permittivity [37], [56], [57], close to 74 at the body temperature [58], and it decreases as the frequency increases. Water also has a low relative imaginary-part permittivity below 1 GHz, close to 4 [56], and increases gradually as the frequency increases to a peak value around 10 GHz, after which it starts to decrease. The literature showed that at 40 °C, slightly higher than the normal body temperature, the complex permittivity was measured as 72.81–j2.254 at

When designing the tuned loop resonator, the dielectric properties of the skin need to be considered.

925 MHz [59]. Considering the high percentage of water in cells and also the high dielectric constant around 1 GHz, changes in water percentage can significantly alter the effective dielectric constant experienced by a resonator or antenna. The lower dielectric loss allows for a higher quality factor in a resonant circuit. The combined effect enables the use of resonant frequency shifts to detect water content changes.

However, the aforementioned argument considers the case of pure water. With a high salt, NaCl, a concentration of 35 g/L in seawater, the real part of relative permittivity decreases slightly to roughly 71, while the dielectric loss increases significantly to approximately 60 [60]. In a typical human body, the sodium concentration is 140 mmol/L (3.22 g/L) in the extracellular fluid and 10 mmol/L (0.23 g/L) in the intracellular fluid when the concentration gradient across the cell membrane is kept by the electrogenic transmembrane adenosine triphosphatases sodium-potassium pump [61]. The fields at 1 GHz take effect both inside and outside the cells because the signals can penetrate cell membranes as the frequency is within the delta dispersion range [34]. Considering the average concentration of sodium in the body, it is roughly 12.5% of that in seawater, and the dielectric loss will be not so much

that it eliminates resonance in the delta dispersion frequency range. However, some effect on quality factors of resonance should be expected.

HYDRATION SENSING BY A RESONATOR

A planar loop resonator on a flexible substrate as a wearable on the forearm to detect hydration levels was developed by our group [62], as shown in Figure 4(a). The resonant frequency is chosen around 1 GHz for the aforementioned reasons. Loop antennas and resonators have been widely used with established analytical formulas to predict resonance [63]. Loop resonators are suitable to be implemented on planar flexible substrates so that they can conform firmly to the skin. However, their quality factors remain low. With the intention to improve resonance, a tuning metal pad is added in the center of the loop to provide distributed reactance to tune its impedance [64]. The results show that tuning the gap, depicted in Figure 4(b), between the ring and center pad, providing adjustable distributed capacitance and mutual inductance, can effectively enhance quality factors from ~5 to 120 in the air at the first-, second- or third-order resonance. The self-tuning structure does not increase the footprint of the sensor, unlike the resonators that use external matching circuits. The distributed reactance tuning along the loop makes the resonator behave like a matched transmission line and enables a robust resonance.

When designing the tuned loop resonator, the dielectric properties of the skin need to be considered. Although the data of wet and dry skins have been documented [65], the permittivities and conductivities at the frequencies of interest are generalized and averaged. Using a coaxial dielectric probe (Keysight N1501 A), measured data are compared with the documented ones in Figure 5 [66]. The partially dehydrated and hydrated conditions of the skin that were created for experiments are explained later. The solid lines are the averaged values, with error bars indicating the ranges of

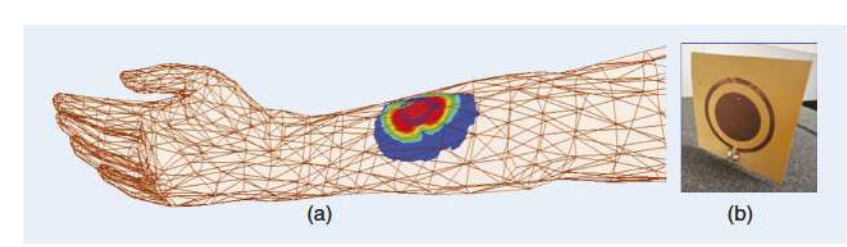


FIGURE 4. (a) Planar tuned loop resonator on a flexible substrate as a wearable on the human forearm to monitor hydration levels. In this illustration, the colors show field distributions at 1 GHz, with the red color being high magnitudes and blue being low magnitudes. The field distributions depend on the sensor's location and tissue properties. An example of field magnitude distributions is in [66]. (b) A photo of the planar tuned loop resonator when it is flat [62], [66].

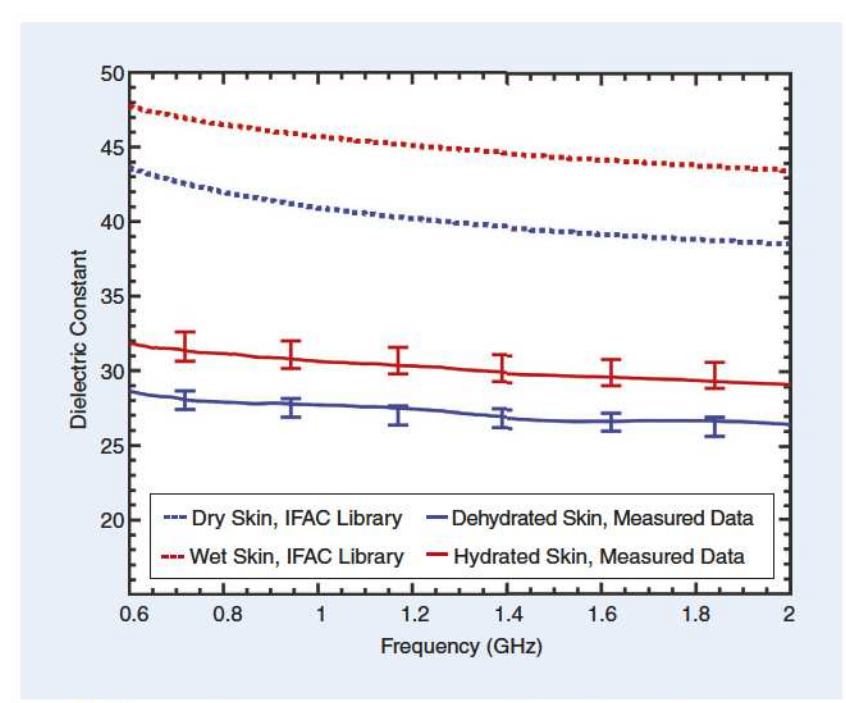


FIGURE 5. Measured dielectric constants of human hydrated and partially dehydrated skins compared with those of wet and dry skins documented in the literature. [65] [Source: International Federation of Automatic Control (IFAC) library.]

data from multiple measurements on the same person. The contact pressures of the probe on the skin were carefully controlled, but it was clear that inconsistent contact can yield measurement variations. When the rigid probe head applied pressure on the tissues, it compressed cells and changed their densities and water distribution inside and among cells. This emphasizes the importance of planar flexible sensors on the skin. Discrepancies between the documented values of permittivity and measured ones are apparent, although the trends in frequency are similar, and the differences between hydrated and dehydrated conditions are distinguishable.

Although the resonator design was conducted with the documented dielectric property of the skin in the literature [65], when the resonator was placed on skin that had different dielectric properties, the robustness of the desired resonance still provided distinct resonant frequency shifts. Figure 6(a) shows the dielectric properties measured with the probe [66]. Figure 6(b) shows the measured responses of the hydrated and dehydrated conditions compared to simulation results using dielectric constants and loss tangents measured by the probe placed next to the resonator. The measured frequency shift was 32 MHz between hydrated and dehydrated conditions, compared to 30 MHz from simulations.

Multiple experiments were conducted for validation [66]. An independent, quick, and quantitative means or instrument, recognized by the clinical community, to characterize total body water loss is not available. It is difficult to create a controlled dehydrating process in a human reliably over a long period of time. When creating a dehydration condition, the safety and health of the subjects must be ensured

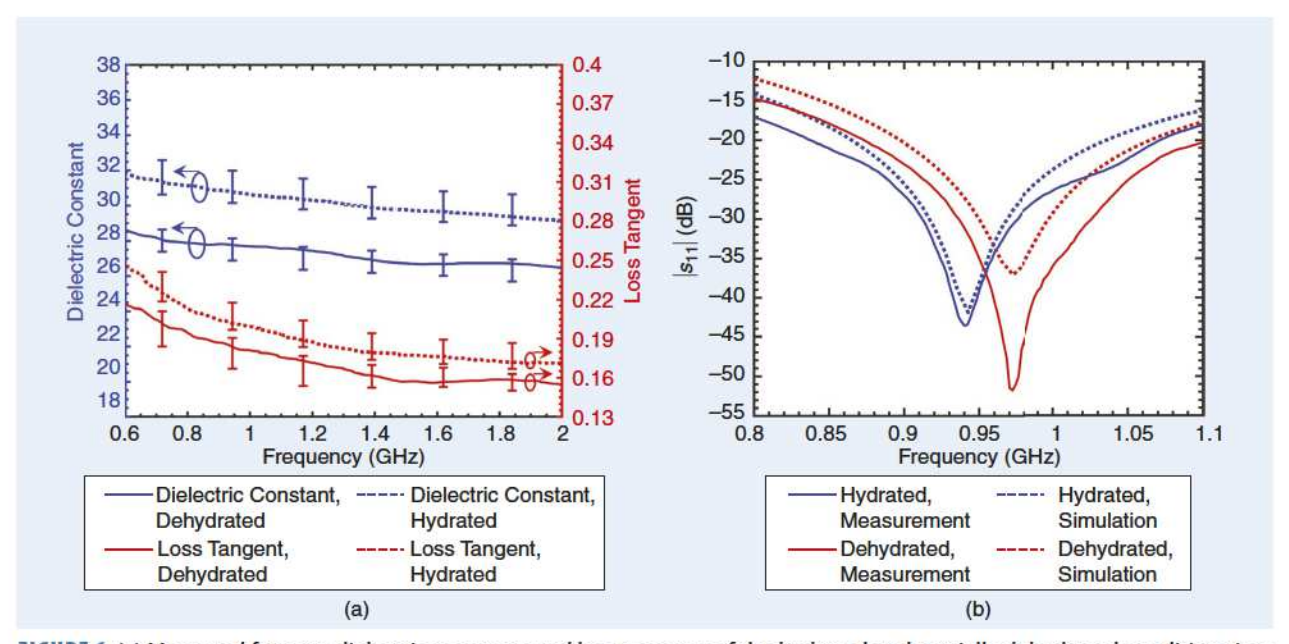


FIGURE 6. (a) Measured forearm dielectric constants and loss tangents of the hydrated and partially dehydrated conditions in a subject. (b) Resonance spectra measured on the hydrated and partially dehydrated forearm skins compared to simulations.

as acute dehydration may cause serious physiological damage. Due to these reasons, we tested the hydration process from a partial dehydration state. The test protocol was implemented in the same fashion for all cases as the following: the subject stopped water, liquid, or food intake after 10 p.m. on the night before the experiment. The next day, at 9 a.m., the person jogged on a treadmill for 45 min to induce sweating. The subject wiped off the sweat and rested until the skin became dry and heartbeat rates/ body temperature returned to the initial values before jogging. By verbal acknowledgment, it was confirmed that the person felt thirsty. Then, the sensor was placed on the inside of the forearm and connected to a vector network analyzer (Keysight PNA N5227B). The subject started to sip water slowly and continued until 1,000 mL of water was consumed. Reflection coefficients, after calibration was done at the sensor connector point, were recorded continuously every 20 s.

Resonant frequencies were sorted out and the shifts were normalized to their final values, as shown in Figure 7 [66]. As the body started getting hydrated, the resonant frequency went back gradually to its plateaued value, which was assumed to be the fully hydrated staMonitoring the dehydration processes was demonstrated with fruits and tissue phantoms made of mixtures of ground pork and saline.

tus in the body. Although the partial dehydration condition was not entirely controllable because of individuals' variations of physiological conditions, the experiments validated the feasibility to record the whole-body hydration level quantitatively. The resonant frequency shifts for partial hydration, with only 50 mL of water consumed after the initial dehydrated state, also showed that the resonance changes were solely due to water intake [66].

Monitoring the dehydration processes was demonstrated with fruits and tissue phantoms made of mixtures of ground pork and saline [67]. The reason to use fruits was that the water could continue evaporating at a constant rate through a designated area, and the results showed a 7% frequency shift over 15 h [66]. Packed ground pork with fat and added saline in a cube volume had a more realistic composi-

tion of tissues. However, the designated surface for water evaporation got hardened after 6–10 h due to the oxidation of fat, and water evaporation was blocked and its rate decreased dramatically. During the initial 8 h of dehydration, 3%–10.5% frequency

shifts were measured. The frequency shifts also showed a linear trend with time. After 8 h, with the dehydration rates slowing down, the frequency shifts still respond to the water losses monotonically [66]. These demonstrations show that the resonant frequency shifts correspond to the water loss percentages in a mass. They also indicate the importance of reliable phantom models for standardized comparison.

Due to the high quality factor provided by the resonator and the tunability of resonance for a specific frequency band and/or material permittivities, similar tuned loop resonators were used in noninvasive subcutaneous probing to identify the boundaries between healthy and abnormal tissues under the skin [68], [69]. These works validated the robustness of the resonators as they could be applied to a wide range of permittivities. The driving power into the resonator connector was set at 10 mW in the experiments. Most of the power went into the tissues, while the rest went into the air. Simulations reveal that the electromagnetic fields around 900 MHz decay by 10 and 20 dB at depths of 5 and 18 mm, respectively, from the skin surface [66]. Fields are thus considered mostly confined in a cylinder volume with a diameter of 4 cm and a depth of 18 mm. Resonance is then mainly determined by the effective permittivities in this specific area that covers both the dermis and hypodermis layers without energy penetrating deeper into the body, which may raise safety concerns. With a high quality factor in resonance, measurable resonant frequency shifts are more sensitive to effective permittivity changes, so field magnitudes and powers can be limited. Further investigation on the specific absorption rate by the tissue mass with respect to different driving powers will

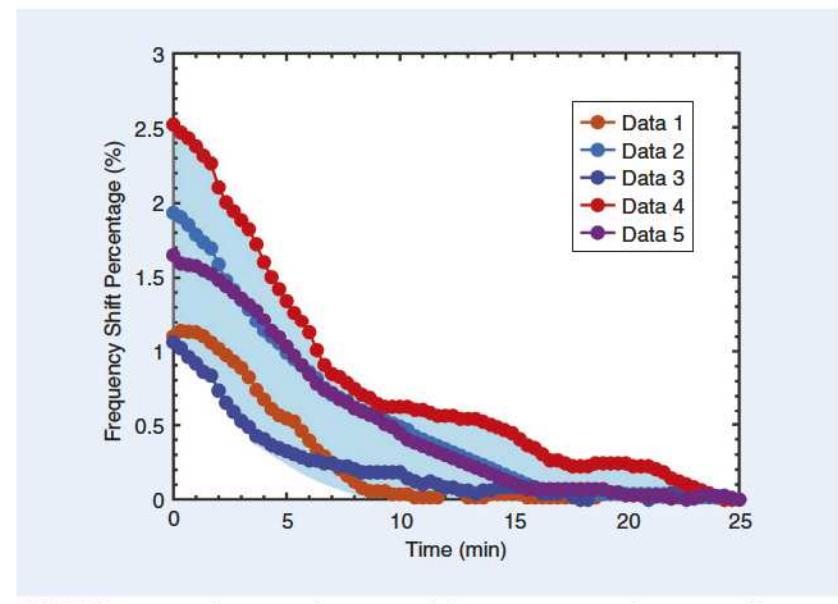


FIGURE 7. Measured resonant frequency shift in percentage when a partially dehydrated person started getting hydrated. Five individual experiments were conducted. The frequency shifts were normalized to the final resonant frequency when the subject was considered to be fully hydrated [66].

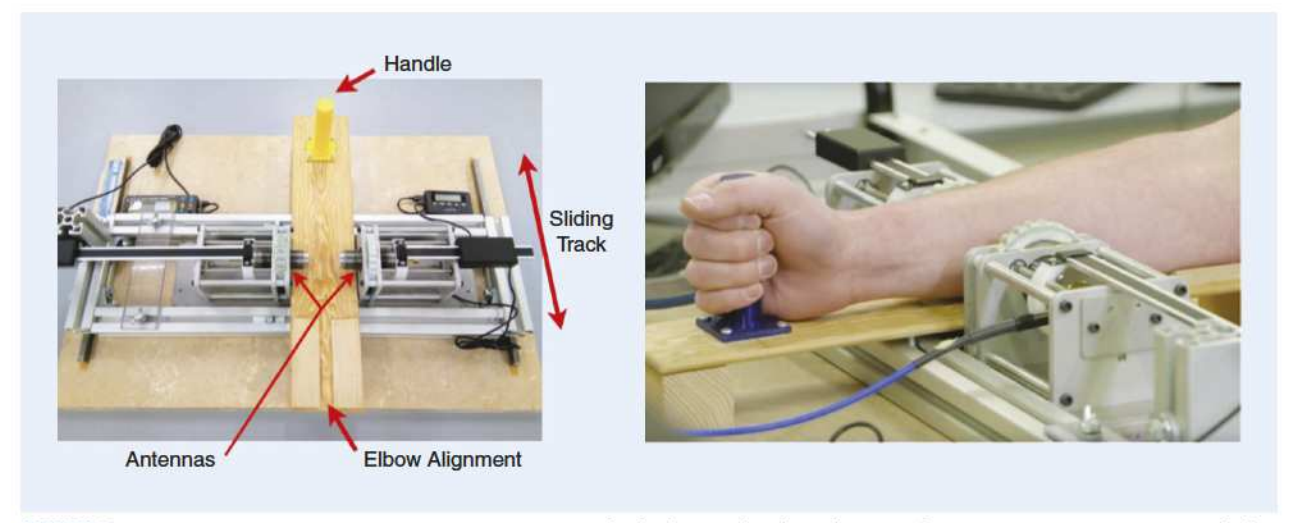


FIGURE 8. A microwave transmission measurement system for hydration-level evaluation. The antennas are in contact with the skin at the midpoint of the forearm. (Source: Garrett et al. in the graphical abstract of [71].)

be needed to determine the safety level in applications.

TRANSMISSION AND REFLECTION SENSING METHODS

A different strategy to assess whole-body hydration levels was demonstrated with a transmission system where microwave signals pass through the human forearm [70], [71]. Two ultrawideband shielded and dielectric-loaded antennas sandwiched a forearm in direct contact with the skin, as shown in Figure 8. Reflection and transmission coefficients at 10 MHz-10 GHz were recorded, and average permittivities were calculated using a time-of-flight (TOF) approach. The signals were converted in the time domain, and the pulse arrival time was found at the maximum of the pulse envelope. Permittivity was then estimated from the difference in arrival time between tissue and air measurements with the same antenna separation distance. The measurements in the midpoint of forearms were conducted on wrestlers before and after their training sessions, along with a control group of subjects. The wrestlers drank water during the sessions. Their weights were recorded and urine samples were measured via urine-specific gravity for comparison. It was concluded that the average estimated permittivity changed 1.43% for each 1% weight change due to water loss; and permittivity was related to water loss, while electric conductivity was less sensitive to changes in water content [69]. The transmission measurements allow assessment of overall effects on permittivity by water content, however, high attenuation due to thick arms prevents accurate TOF analysis. The physical configuration of the measurement setup also prevents real-time continuous measurements, making it challenging to become a wearable.

Controlled experiments on the body to study specific microwave effects by water content are difficult to manage and are made more so by sophisticated internal mechanisms that human and animal bodies have to regulate hydration in tissues. These challenges are manifested in the human experiments mentioned previously. It is also difficult to create chronic dehydration conditions in the body without harming subjects. Thus, creating realistic phantoms to mimic hydration levels becomes important.

Brendtke et al. [72] demonstrated hydration-level measurements using microwave return losses on skin equivalents made of specific hydration and density of compressed matrix components, such as collagen type 1 hydrogel, cultured cells, and reagents. The osmolality of skin equivalents was altered by incubating the tissue samples in NaCl at different concentrations or in purified water to mimic dehydration levels. A broadband (7–9 GHz) patch antenna, fabricated on a hydrocarbon ceramic laminate (RO4350, Rogers Corp.), was

optimized at 7.9 GHz and connected to a vector network analyzer from the backside. The measurement volume was 3.6 cm³, although the dimensions and radiation pattern of the patch antenna and the port calibration method were not disclosed in [72]. The antenna was placed facing the skin-equivalent model confined in a chamber, as shown in Figure 9. The return loss and the frequency where the minimum loss occurred were obtained from emission (0.631 mW) and reflection powers in the spectrum of 7-9.5 GHz. Feasibility study results showed that shifts of the frequency at the local minimum of the return loss and the local return loss at a fixed frequency (at 8.2 GHz in [72]) could be used as osmolality readings. The skin equivalents may serve as a

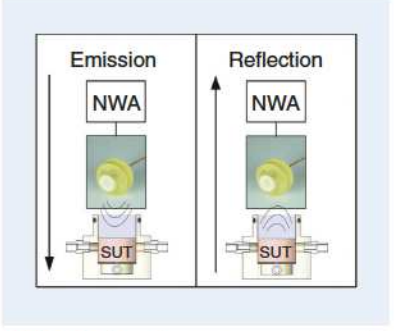


FIGURE 9. A patch antenna connected to a network analyzer (NWA) emits signals into the substance-under-test (SUT) chamber and detects reflection signals in the frequency range of 7–9 GHz. Courtesy of Brendtke et al. [72].

standard for sensor performance evaluation in the future.

CONCLUSIONS AND FUTURE OUTLOOK

This review presented an overview of continuous hydration/dehydration evaluations on the human body and their principles, including radio-frequency impedance techniques and microwave measurements through the skin. The review focused on the techniques that are suitable for wearables. It is indisputable that acute and chronic dehydration leads to many physical and mental health problems. A convenient, comfortable, continuous, real-time, quantitative, and accurate hydration monitor that can be worn on the body can benefit many people and empower personalized health care. However, the difficulty to create quantitively controlled and repeatable environments for total body water measurements in humans and phantoms, even after incorporating the advances discussed in this article, leaves tremendous challenges for the study and development of wearable, noninvasive hydration sensors. Experimental protocols for hydration assessment for humans and measurement phantoms need refinement and standardization to further advance the state of the art for device designs.

Bioimpedance provides insights into moisture levels at the top layer of the skin. The impedance measurements conducted with capacitive and/or resistive electrodes can be implemented on conformable substrates on the skin. Microwaves probe deeper into the dermis and hypodermis layers, where fields can interact more directly with water content because of blood vessels and sweat glands in the layers. The response is quicker as the fields react to the water in the blood and interstitial fluids. Tuned loop resonators can be made on planar flexible wearables attached to limbs. The sharp resonance provides sensitive responses to hydration-level changes. Transmission and reflection measurements with a waveguide that covers thicker tissue layers may give a more precise assessment of the wholebody water content but are too large for wearable applications. Coaxial probes provide a wider bandwidth, allowing a better evaluation of the permittivities of tissues across frequencies of interest. Their instrumentation for wearables needs further design consideration. Ultrawideband spectroscopy that detects both the impedances and scattering coefficients may give us more information about the overall dehydration status.

Although dielectric property characterizations on specific human tissues have been documented, they present mostly statistically averaged values. The dielectric properties of individuals' skins and tissues vary significantly from person to person, and a person's hydration status is related to the entire body system. Therefore, individualized calibration and signal processing mechanisms for noninvasive electromagnetic-wave probing on a local area to evaluate whole-body hydration levels may benefit from machine learning techniques. Device designs, especially for planar conformable wearables, that meet the requirements of multiple operating frequencies, bandwidths, limited powers, high sensitivity to dielectric properties, and substrate materials, require more work before they can be considered for reliable, cost-effective, and personalized uses.

ACKNOWLEDGMENT

We wish to thank the support of the National Science Foundation under Grant ENG-CMMI-1929953 for the work conducted in the section "Hydration Sensing by a Resonator" of this article.

This work involved human subjects in its research. Approval of all ethical and experimental procedures and protocols was granted by the Southern Methodist University Institutional Review Board committee on 19 April 2021 and performed in line with Human Subjects Research Protocol H21-023-CHIJ.

AUTHOR INFORMATION

J.-C. Chiao (jchiao@smu.edu) is with the Department of Electrical and Computer Engineering, Southern Methodist University, Dallas, TX 75205 USA. He is a Fellow of IEEE. Sen Bing (sbing@smu.edu) is with the Department of Electrical and Computer Engineering, Southern Methodist University, Dallas, TX 75205 USA. He is a Member of IEEE.

Khengdauliu Chawang (kchawang @smu.edu) is with the Department of Electrical and Computer Engineering, Southern Methodist University, Dallas, TX 75205 USA. He is a Graduate Student Member of IEEE.

Brian Crowe (brian_crowe@i-worx. com) is with Tele-Worx, Grand Prairie TX 75050 USA. He is a Life Senior Member of IEEE.

REFERENCES

- [1] G. Arnaoutis et al., "The effect of hypohydration on endothelial function in young healthy adults," Eur. J. Nutr., vol. 56, no. 3, pp. 1211–1217, 2017, doi: 10.1007/s00394-016-1170-8.
- [2] J. C. Watso and W. B. Farquhar, "Hydration status and cardiovascular function," *Nutrients*, vol. 11, no. 8, 2019, Art. no. 1866, doi: 10.3390/ nu11081866.
- [3] S. Green and B. Dawson, "Measurement of anaerobic capacities in humans: Definitions, limitations and unsolved problems," Sports Med., vol. 15, no. 5, pp. 312–327, 1993, doi: 10.2165/00007256 -199315050-00003.
- [4] L. C. Jones, M. A. Cleary, R. M. Lopez, R. E. Zuri, and R. Lopez, "Active dehydration impairs upper and lower body anaerobic muscular power," J. Strength Conditioning Res., vol. 22, no. 2, pp. 455–463, 2008, doi: 10.1519/JSC.0b013e3181635ba5.
- [5] I. Martínez-Navarro, A. Montoya-Vieco, E. Collado, B. Hernando, N. Panizo, and C. Hernando, "Muscle cramping in the marathon: Dehydration and electrolyte depletion vs. muscle damage," J. Strength Conditioning Res., vol. 36, no. 6, pp. 1629–1635, 2022, doi: 10.1519/JSC.00000000000003713.
- [6] A. Kahn, E. Brachet, and D. Blum, "Controlled fall in natremia and risk of seizures in hypertonic dehydration," *Intensive Care Med.*, vol. 5, no. 1, pp. 27–31, 1979, doi: 10.1007/BF01738999.
- [7] R. D. Andrew, "Seizure and acute osmotic change: Clinical and neurophysiological aspects," J. Neurol. Sci., vol. 101, no. 1, pp. 7–18, 1991, doi: 10.1016/0022-510X(91)90013-W.
- [8] L. E. Armstrong et al., "Mild dehydration affects mood in healthy young women," J. Nutr., vol. 142, no. 2, pp. 382–388, 2012, doi: 10.3945/ jn.111.142000.
- [9] A. C. Grandjean and N. R. Grandjean, "Dehydration and cognitive performance," J. Am. Coll. Nutr., vol. 26, pp. 5498–5548, Jul. 2013, doi: 10.1080/07315724.2007.10719657.
- [10] M. M. Wilson and J. Morley, "Impaired cognitive function and mental performance in mild dehydration," *Eur. J. Clin. Nutr.*, vol. 57, pp. S24– S29, Dec. 2003, doi: 10.1038/sj.ejcn.1601898.
- [11] M. Nagae et al., "Chronic dehydration in nursing home residents," *Nutrients*, vol. 12, no. 11, 2020, Art. no. 3562, doi: 10.3390/nu12113562.
- [12] C. L. Chapman, B. D. Johnson, N. T. Vargas, D. Hostler, M. D. Parker, and Z. J. Schlader, "Both hyperthermia and dehydration during physical

- work in the heat contribute to the risk of acute kidney injury," *J. Appl. Physiol.*, vol. 128, no. 4, pp. 715–728, 2020, doi: 10.1152/japplphystol. 00787.2019.
- [13] C. Roncal-Jimenez, M. A. Lanaspa, T. Jensen, L. G. Sanchez-Lozada, and R. J. Johnson, "Mechanisms by which dehydration may lead to chronic kidney disease," Ann. Nutr. Metab., vol. 66, no. Suppl. 3, pp. 10–13, 2015, doi: 10.1159/000381239.
- [14] G. F. Strippoli, J. C. Craig, E. Rochtchina, V. M. Flood, J. J. Wang, and P. Mitchell, "Fluid and nutrient intake and risk of chronic kidney disease," *Nephrology*, vol. 16, no. 3, pp. 326–334, 2011, doi: 10.1111/j.1440-1797.2010.01415.x.
- [15] K. Lean, R. F. Nawaz, S. Jawad, and C. Vincent, "Reducing urinary tract infections in care homes by improving hydration," *BMJ Open Qual.*, vol. 8, no. 3, 2019, Art. no. e000563, doi: 10.1136/bmjoq-2018-000563.
- [16] R. Beetz, "Mild dehydration: A risk factor of urinary tract infection?" Eur. J. Clin. Nutr., vol. 57, pp. S52–S58, Dec. 2003, doi: 10.1038/ sj.ejcn.1601902.
- [17] M. Frangeskou, B. Lopez-Valcarcel, and L. Serra-Majem, "Dehydration in the elderly: A review focused on economic burden," *J. Nutr. Health Aging*, vol. 19, no. 6, pp. 619–627, 2015, doi: 10.1007/s12603-015-0491-2.
- [18] C. Duggan, M. Refat, M. Hashem, M. Wolff, I. Fayad, and M. Santosham, "How valid are clinical signs of dehydration in infants?" J. Pediatr. Gastroenterol. Nutr., vol. 22, no. 1, pp. 56–61, 1996, doi: 10.1097/00005176-199601000-00009.
- [19] E. D. Goulet, "Dehydration and endurance performance in competitive athletes," Nutr. Rev., vol. 70, pp. S132–S136, Nov. 2012, doi: 10.1111/j.1753-4887.2012.00530.x.
- [20] P. Acharya, B. Boggess, and K. Zhang, "Assessing heat stress and health among construction workers in a changing climate: A review," Int. J. Environ. Res. Public Health, vol. 15, no. 2, 2018, Art. no. 247, doi: 10.3390/ijerph15020247.
- [21] N. López-Gálvez et al., "Longitudinal assessment of kidney function in migrant farm workers," *Environ. Res.*, vol. 202, Nov. 2021, Art. no. 111686, doi: 10.1016/j.envres.2021.111686.
- [22] F. Trenz, R. Weigel, and A. Hagelauer, "Methods for human dehydration measurement," Frequenz, vol. 72, nos. 3–4, pp. 159–166, 2018, doi: 10.1515/freq-2018-0006.
- [23] L. E. Armstrong, "Hydration assessment techniques," Nutr. Rev., vol. 63, pp. S40–S54, Jun. 2005, doi: 10.1111/j.1753-4887.2005.tb00153.x.
- [24] L. A. Popowski, R. A. Oppliger, P. Lambert, R. F. Johnson, and C. V. Gisolf, "Blood and urinary measures of hydration status during progressive acute dehydration," *Med. Sci. Sports Exercise*, vol. 33, no. 5, pp. 747–753, 2001, doi: 10.1097/00005768-200105000-00011.
- [25] L. E. Armstrong, J. A. H. Soto, F. T. Hacker, D. J. Casa, S. A. Kavouras, and C. M. Maresh, "Urinary indices during dehydration, exercise, and rehydration," *Int. J. Sport Nutr. Exercise Metab.*, vol. 8, no. 4, pp. 345–355, 1998, doi: 10.1123/ijsn.8.4.345.
- [26] L. Hooper et al., "Diagnostic accuracy of calculated serum osmolarity to predict dehydration in older people: Adding value to pathology laboratory reports," *BMJ Open*, vol. 5, no. 10, 2015, Art. no. e008846, doi: 10.1136/bmjopen-2015-008846.
- [27] B. Schazmann et al., "A wearable electrochemical sensor for the real-time measurement of sweat sodium concentration," *Anal. Methods*, vol. 2, no. 4, pp. 342–348, 2010, doi: 10.1039/B9AY00184K.

- [28] D. P. Rose et al., "Adhesive RFID sensor patch for monitoring of sweat electrolytes," *IEEE Trans. Biomed. Eng.*, vol. 62, no. 6, pp. 1457–1465, Jun. 2014, doi: 10.1109/TBME.2014.2369991.
- [29] V. Dam, M. Zevenbergen, and R. Van Schaijk, "Flexible chloride sensor for sweat analysis," Procedia Eng., vol. 120, pp. 237–240, Sep. 2015, doi: 10.1016/j.proeng.2015.08.588.
- [30] M. Y. Jaffrin and H. Morel, "Body fluid volumes measurements by impedance: A review of bioimpedance spectroscopy (BIS) and bioimpedance analysis (BIA) methods," *Med. Eng. Phys.*, vol. 30, no. 10, pp. 1257–1269, 2008, doi: 10.1016/j.medengphy.2008.06.009.
- [31] S. S. Sun et al., "Development of bioelectrical impedance analysis prediction equations for body composition with the use of a multicomponent model for use in epidemiologic surveys," Am. J. Clin. Nutr., vol. 77, no. 2, pp. 331–340, 2003, doi: 10.1093/ajcn/77.2.331.
- [32] U. G. Kyle, L. Genton, L. Karsegard, D. O. Slosman, and C. Pichard, "Single prediction equation for bioelectrical impedance analysis in adults aged 20–94 years," Nutrition, vol. 17, no. 3, pp. 248–253, 2001, doi: 10.1016/S0899-9007(00)00553-0.
- [33] B. R. Patil, D. P. Patkar, S. A. Mandlik, M. M. Kuswarkar, and G. D. Jindal, "Single prediction equation for bioelectrical impedance analysis in adults aged 22–59 years," J. Med. Eng. Technol., vol. 35, no. 2, pp. 109–114, 2011, doi: 10.3109/03091902.2010.543751.
- [34] H. P. Schwan, "Electrical properties of tissue and cell suspensions," in Advances in Biological and Medical Physics, J. H. Lawrence and C. A. Tobias, Eds., Amsterdam, The Netherlands: Elsevier, 1957, pp. 147–209.
- [35] S. M. Neuder, "Electromagnetic fields in biological media," US Dept. Health, Educ., Welfare, Public Health Service, Food Drug Admin., Bur. Radiological Health, Rockville, MD, USA, Tech. Rep. FDA-78-8068, 1978.
- [36] N. Nasir and M. Al Ahmad, "Cells electrical characterization: Dielectric properties, mixture, and modeling theories," J. Eng., vol. 2020, pp. 1–17, Jan. 2020, doi: 10.1155/2020/9475490.
- [37] C. Gabriel, "Dielectric properties of biological materials," in *Handbook of Biological Effects of Electromagnetic Fields*, F. S. Barnes and B. Greenebaum, Eds., New York, NY, USA: CRC Press, 2006, pp. 51–100.
- [38] X. Huang et al., "Materials and designs for wireless epidermal sensors of hydration and strain," Adv. Funct. Mater., vol. 24, no. 25, pp. 3846–3854, 2014, doi: 10.1002/adfm.201303886.
- [39] X. Huang, W. Yeo, Y. Liu, and J. A. Rogers, "Epidermal differential impedance sensor for conformal skin hydration monitoring," *Biointerphases*, vol. 7, no. 1, 2012, Art. no. 52, doi: 10.1007/s13758 -012-0052-8.
- [40] S. Yao et al., "A wearable hydration sensor with conformal nanowire electrodes," Adv. Healthcare Mater., vol. 6, no. 6, 2017, Art. no. 601159, doi: 10.1002/adhm.201601159.
- [41] A. M. Campbell, Measurements and Analysis of the Microwave Dielectric Properties of Tissues. Glasgow, Scotland: Univ. of Glasgow, Oct. 1990.
- [42] R. Pethig, "Dielectric properties of biological materials: Biophysical and medical applications," *IEEE Trans. Elect. Insul.*, vol. EI-19, no. 5, pp. 453–474, Oct. 1984, doi: 10.1109/TEI.1984. 298769.
- [43] S. Singh, R. K. Tiwari, V. Sood, R. Kaur, and S. Prashar, "The legacy of scatterometers: Review of applications and perspective," *IEEE Geosci.*

- Remote Sens. Mag., vol. 10, no. 2, pp. 39–65, Jun. 2022, doi: 10.1109/MGRS.2022.3145500.
- [44] Y. H. Kerr, P. Waldteufel, J. Wigneron, J. Martinuzzi, J. Font, and M. Berger, "Soil moisture retrieval from space: The soil moisture and ocean salinity (SMOS) mission," *IEEE Trans. Geosci. Remote Sens.*, vol. 39, no. 8, pp. 1729–1735, Aug. 2001, doi: 10.1109/36.942551.
- [45] N. Reul, J. Tenerelli, B. Chapron, D. Vandemark, Y. Quilfen, and Y. Kerr, "SMOS satellite l-band radiometer: A new capability for ocean surface remote sensing in hurricanes," J. Geophys. Res. Oceans, vol. 117, no. C2, 2012, doi: 10.1029/2011JC007474.
- [46] D. Entekhabi et al., "The soil moisture active passive (SMAP) mission," *Proc. IEEE*, vol. 98, no. 5, pp. 704–716, May 2010, doi: 10.1109/ JPROC.2010.2043918.
- [47] J. Wigneron et al., "Modelling the passive microwave signature from land surfaces: A review of recent results and application to the L-band SMOS & SMAP soil moisture retrieval algorithms," *Remote Sens. Environ.*, vol. 192, pp. 238–262, Apr. 2017, doi: 10.1016/j.rse.2017.01.024.
- [48] B. Bauer-Marschallinger et al., "Toward global soil moisture monitoring with sentinel-1: Harnessing assets and overcoming obstacles," *IEEE Trans. Geosci. Remote Sens.*, vol. 57, no. 1, pp. 520–539, Jan. 2019, doi: 10.1109/TGRS.2018.2858004.
- [49] Z. Sokol, J. Szturc, J. Orellana-Alvear, J. Popová, A. Jurczyk, and R. Célleri, "The role of weather radar in rainfall estimation and its application in meteorological and hydrological modelling—A review," *Remote Sens.*, vol. 13, no. 3, pp. 351, 2021, doi: 10.3390/rs13030351.
- [50] C. Wohlfart, K. Winkler, A. Wendleder, and A. Roth, "TerraSAR-X and wetlands: A review," Remote Sens., vol. 10, no. 6, 2018, Art. no. 916, doi: 10.3390/rs10060916.
- [51] S. Buckreuss et al., "Ten years of TerraSAR-X operations," *Remote Sens.*, vol. 10, no. 6, 2018, Art. no. 873. doi: 10.3390/rs10060873.
- [52] L. Brocca et al., "A review of the applications of ASCAT soil moisture products," *IEEE J. Sel. Topics Appl. Earth Observ. Remote Sens.*, vol. 10, no. 5, pp. 2285–2306, May 2017, doi: 10.1109/ JSTARS.2017.2651140.
- [53] S. Singh, R. K. Tiwari, H. S. Gusain, and V. Sood, "Potential applications of SCATSAT-1 satellite sensor: A systematic review," *IEEE Sensors J.*, vol. 20, no. 21, pp. 12,459–12,471, Nov. 2020, doi: 10.1109/JSEN.2020.3002720.
- [54] A. Guyton, Textbook of Medical Physiology, 5th ed. Philadelphia, PA, USA: W.B. Saunders, 1976.
- [55] H. H. Mitchell, T. Hamilton, F. Steggerda, and H. Bean, "The chemical composition of the adult human body and its bearing on the biochemistry of growth," J. Biol. Chem., vol. 158, no. 3, pp. 625– 637, 1945, doi: 10.1016/S0021-9258(19)51339-4.
- [56] J. B. Hasted, "Liquid water: Dielectric properties," in *The Physics and Physical Chemistry of Water*, F. Franks. Ed., 1972, pp. 255–309.
- [57] R. Buchner, J. Barthel, and J. Stauber, "The dielectric relaxation of water between 0 C and 35 C," Chem. Phys. Lett., vol. 306, nos. 1–2, pp. 57–63, 1999, doi: 10.1016/S0009-2614(99)00455-8.
 [58] D. G. Archer and P. Wang, "The dielectric constant of water and Debye-Hückel limiting law slopes," J. Phy. Chem. Ref. Data, vol. 19, no. 2, pp. 371–411, 1990, doi: 10.1063/1.555853.
- [59] P. O. Risman and B. Wäppling-Raaholt, "Retromodelling of a dual resonant applicator and accurate dielectric properties of liquid water from -20°C to 100°C," Meas. Sci. Technol., vol. 18, no. 4, 2007, Art. no. 959, doi: 10.1088/0957-0233/18/4/001.

[60] T. Meissner and F. J. Wentz, "The complex dielectric constant of pure and sea water from microwave satellite observations," *IEEE Trans. Geosci. Remote Sens.*, vol. 42, no. 9, pp. 1836–1849, Sep. 2004, doi: 10.1109/TGRS.2004.831888.
[61] P. Strazzullo and C. Leclercq, "Sodium," *Adv. Nutr.*, vol. 5, no. 2, pp. 188–190, 2014, doi: 10.3945/an.113.005215.

[62] S. Bing, K. Chawang, and J. Chiao, "A resonant coupler for subcutaneous implant," Sensors, vol. 21, no. 23, 2021, Art. no. 8141, doi: 10.3390/s21238141.

[63] A. F. McKinley, T. P. White, I. S. Maksymov, and K. R. Catchpole, "The analytical basis for the resonances and anti-resonances of loop antennas and meta-material ring resonators," *J. Appl. Phys.*, vol. 112, no. 9, 2012, Art. no. 094911, doi: 10.1063/ 1.4764104.

[64] S. Bing, K. Chawang, and J. Chiao, "A self-tuned method for impedance-matching of planar-loop resonators in conformable wearables," *Electronics*, vol. 11, no. 17, 2022, Art. no. 2784, doi: 10.3390/electronics11172784.

[65] D. Andreuccetti, R. Fossi, and C. Petrucci. "An Internet resource for the calculation of the dielectric properties of body tissues in the frequency range 10 Hz-100 GHz." NirEmf. Accessed: Sep. 1, 2023. [Online]. Available at: http://niremf.ifac.cnr.it/tissprop/

[66] S. Bing, K. Chawang, and J. Chiao, "A flexible tuned radio-frequency planar resonant loop for noninvasive hydration sensing," *IEEE J. Micro*waves, vol. 3, no. 1, pp. 181–192, Jan. 2023, doi: 10.1109/JMW.2022.3224087.

[67] S. Bing, K. Chawang, and J. Chiao, "A radio-frequency planar resonant loop for noninvasive monitoring of water content," in *Proc. IEEE Sensors*, Dallas, TX, USA, 2022, pp. 1–4, doi: 10.1109/SENSORS52175.2022.9967154.

[68] S. Bing, K. Chawang, and J.-C. Chiao, "A tuned microwave resonant system for subcutaneous imaging," Sensors, vol. 23, no. 6, 2023, Art. no. 3090, doi: 10.3390/s23063090.

[69] S. Bing, K. Chawang, and J.-C. Chiao, "A tuned microwave resonant sensor for skin cancerous tumor diagnosis," *IEEE J. Electromagn.*, RF Microw. Med. Biol., vol. 7, no. 4, pp. 320–327, Dec. 2023, doi: 10.1109/JERM.2023.3281726.

[70] D. C. Garrett and E. C. Fear, "Feasibility study of hydration monitoring using microwaves – Part 1: A model of microwave property changes with dehydration," *IEEE J. Electromagn., RF Microw. Med. Biol.*, vol. 3, no. 4, pp. 292–299, Dec. 2019, doi: 10.1109/JERM. 2019.2911849.

[71] D. C. Garrett, J. R. Fletcher, D. B. Hogan, T. S. Fung, and E. C. Fear, "Feasibility study of hydration monitoring using microwaves – Part 2: Measurements of athletes," *IEEE J. Electromagn.*, RF Microw. Med. Biol., vol. 3, no. 4, pp. 300–307, Dec. 2019, doi: 10.1109/JERM.2019.2911909.

[72] R. Brendtke, M. Wiehl, F. Groeber, T. Schwarz, H. Walles, and J. Hansmann, "Feasibility study on a microwave-based sensor for measuring hydration level using human skin models," *PLoS One*, vol. 11, no. 4, 2016, Art. no. e0153145, doi: 10.1371/journal.pone.0153145.



MEETINGS & SYMPOSIA (continued from page 64)

19th EUROPEAN CONFERENCE ON ANTENNAS AND PROPAGATION (EuCAP 2025)

30 March—4 April 2025, Stockholm, Sweden. (Papers: 18 October 2024). The European Association on Antennas and Propagation, 86c Avenue du Port, Box 204, 1000 Brussels, Belgium. e-mail: info@eucap2024.org. https://www.eucap2025.org/.

WIRELESS, ANTENNA, AND MICROWAVE SYMPOSIUM (WAMS 2025)

5–8 June 2025, Kancheepuram, Chennai, India. (Papers: 31 December 2024). Contacts: M.D. Selvara, general chair,

+91 9941524269; e-mail: selvaraj@iiitdm.ac.in; Srijith K., organizing chair, +91 9444165638; e-mail: srijith@iiitdm.ac.in. http://www.wams2025.iiitdm.ac.in/.

IEEE INTERNATIONAL CONFERENCE ON COMMUNICATIONS (ICC 2025)

8–12 June 2025, Montreal, Canada. (Papers: 11 October 2024). Melissa Torres, senior conference planner, IEEE Communications Society, +1 212 705 8979; e-mail: m.a.torres@comsoc.org. http://icc2025.ieee-icc.org.



COURSES (continued from page 65)

TEST AND EVALUATION OF RF SYSTEMS

25–27 February 2025, ONLINE. Georgia Institute of Technology, Professional Education, P.O. Box 93686, Atlanta, GA 30377-0686, USA. +1 404 385-3500, fax: +1 404 894-8925. http://www.pe.gatech.edu.

SIGNALS INTELLIGENCE (SIGINT) FUNDAMENTALS 4–5 March 2025, Denver, CO, USA.

MODERN ELECTRONIC AND DIGITAL SCANNED ARRAY ANTENNAS

17–21 March 2025, San Diego, CA, USA. Georgia Institute of Technology, Professional Education, P.O. Box 93686, Atlanta, GA 30377-0686, USA. +1 404 385-3500, fax: +1 404 894-8925. http://www.pe.gatech.edu.

